# Plasticity and damage with gradient enhancement: A review of application to high speed forming

To cite this article: L Poggenpohl *et al* 2017 *J. Phys.: Conf. Ser.* **896** 012078

View the article online for updates and enhancements.

## Related content

- A numerical analysis on forming limits during spiral and concentric single point incremental forming
  M L Gipiela, V Amauri, C Nikhare et al.

- The Mechanism of Critical Strain of Serrated Yielding in Strain Rate Domain
  Shi-Hua Fu, Yu-Long Cai, Su-Li Yang et al.

- Research on mechanical and sensoric set-up for high strain rate testing of high performance fibers
  R Unger, P Schegner, A Nocke et al.

# Plasticity and damage with gradient enhancement: A review of application to high speed forming

**L Poggenpohl, Y Kiliclar, T Brepols, S Wulfinghoff and S Reese**

Institute of Applied Mechanics, RWTH Aachen University, Mies-van-der-Rohe-Str. 1, 52074 Germany

E-mail: `Lukas.Poggenpohl@ifam.rwth-aachen.de`

**Abstract.** Efficiency, durability and lightweight are key aspects in designing new products such as cars or other machines. However, when materials are processed by plastic forming, one has to consider the forming limits of the materials which indicate the starting point for localization or fracture of the material. High speed forming processes, such as electro-magnetic forming offer a possibility to widen these limits. Since standard plasticity models do not account for the damage behavior at these high strain rates, a new model of coupled damage-plasticity at high strains and high strain rates has to be developed.

When damage occurs, one may have to deal with a mechanism called localization, which leads to non-physical solutions. One way to deal with this problem is to introduce a gradient enhanced damage model. In this paper, a gradient enhanced elasto-plastic model was developed and tested on some academic examples such as notched beams.

## 1. Introduction

In engineering, one always aims at the optimal product in terms of (energy-) efficiency and durability. In many applications, such as car or airplane manufacturing, lightweight design is a direct consequence of energy efficiency requirements. In order to meet these requirements, higher formability is needed to achieve more freedom of design, like sharper edges or lower edge angles. But the ability of a metal, e.g. aluminum alloys, to endure forming is limited. The limits of an alloy to endure irreversible deformation can be shown in a forming limit curve (FLC), where the strain combinations at failure are summarized. In 1950, it was firstly reported by Clark and Wood [1], that high strain rates result into increased forming limits. Due to their findings, high speed forming is suggested to enable the desired higher formability [2].

## 2. Electromagnetic forming

Quasi-static forming is cost efficient but is limited due to relatively small strain rates [3]. Electromagnetic forming on the other hand enables the realization of much higher strain rates, but the process is very energy consuming and therefore expensive. Here, a combination of quasi static and electromagnetic forming will be investigated with respect to deep drawing. The quasi static process of deep drawing is used to perform the main part of the forming process. Critical geometries, which lie outside of the quasi-static forming limits are then formed by an electomagnetic pulse [4].

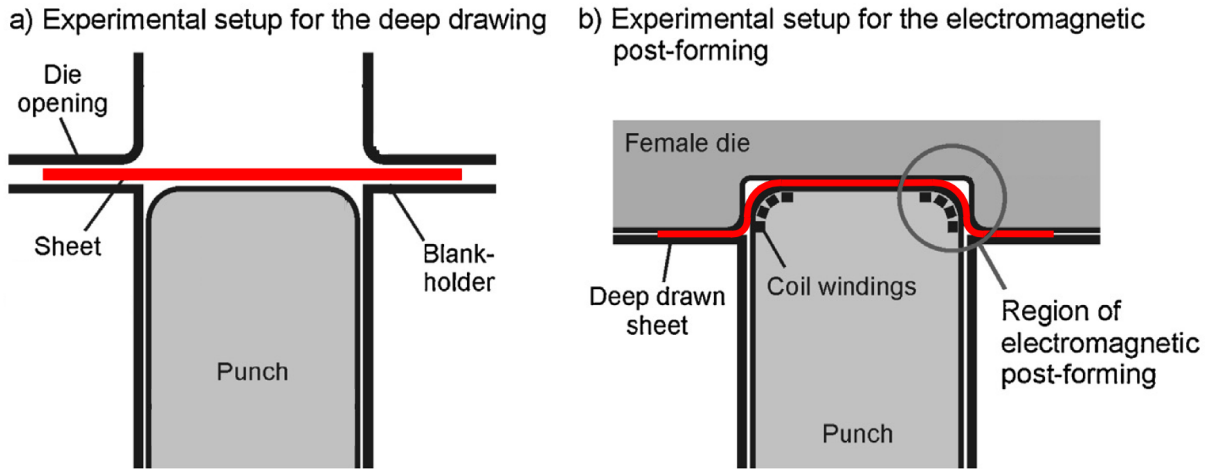In Fig. 1, a possible application is shown. In the first step, the workpiece is deepdrawn. In the

**Figure 1.** Exemplary experimental setup for a combined deep drawing and electomagnetic forming process [3]

second step, electomagnetic forming is used to subsequently form the final edge with a much smaller radius which would not be possible within deep drawing. This combination of quasi static and high speed forming is considered as the optimal solution with respect to formability and cost efficiency [3]. However, one has to adjust the parameters for both processes carefully, if one really wants to extend the quasi static FLC. Therefore it is crucial to gain a systematic scientific understanding of the process.

Material modeling provides the possibility, to gain a profound understanding of the process and the material behavior [5]. Here, a material model is introduced to accurately predict the forming limits under largely varying strain rates. With application of this model to a simulation of the prescribed forming process one then can optimize the process parameters in order to extend the quasi static FLC.

### 2.1. Material modeling

The presented model accounts for the elasto-plastic behavior at different strain rates as well as the damage behavior within the plastic domain. It it based on an extension of the material models of Vladimirov et al. [6] and Dettmer & Reese [7]. Especially rate-dependence is introduced.

For the deformation gradient $\mathbf{F}$ in finite deformations it is assumed that the multiplicative split $\mathbf{F} = \mathbf{F}_e \mathbf{F}_p$ holds. In addition a second split for the plastic part into elastic and inelastic parts is assumed:

$$\mathbf{F}_p = \mathbf{F}_{p_e} \mathbf{F}_{p_i} \tag{1}$$

For each of the parts of the deformation gradient, a right Cauchy-Green tensor $\mathbf{C}_i = \mathbf{F}_i^T \mathbf{F}_i \qquad i \in [e, p_e, p_i]$ can be introduced. The Helmholz free energy for the Armstrong-Frederick model of kinematic hardening in this case reads

$$\psi = \psi_e(\mathbf{C}_e) + \psi_{kin}(\mathbf{C}_{p_e}) + \psi_{iso}(\kappa). \tag{2}$$

Here, $\kappa$ denotes the parameter for isotropic hardening.

Application of Eq. (2) to the Clausius-Duhem inequality (where $\mathbf{S}$ denotes the second Piola-

Kirchhoff stress tensor) yields

$$-\left(\frac{\partial\psi_e}{\partial\mathbf{C}_e}\dot{\mathbf{C}}_e + \frac{\partial\psi_{kin}}{\partial\mathbf{C}_{p_e}}\dot{\mathbf{C}}_{p_e} + \frac{\partial\psi_{iso}}{\partial\kappa}\dot{\kappa}\right) + \mathbf{S}\cdot\frac{1}{2}\dot{\mathbf{C}} \geq 0. \tag{3}$$

A detailed derivation of the evolution equations and the yield function is given in [8]. In the following lines, only the resulting evolution equations will be shown:

The evolution equation for the isotropic hardening variable reads

$$\dot{\kappa} = \dot{\lambda}\frac{\partial\Phi}{\partial R}, \tag{4}$$

where $R$ represents the isotropic hardening stress, given by $R = -\mathcal{Q}(1 - e^{-\beta\kappa})$. In this case, $\mathcal{Q}$ and $\beta$ are material parameters controlling isotropic hardening. In [8] the symmetric part of the inelastic plastic velocity gradient $\mathbf{d}_{p_i}$ is introduced. The evolution equation for this reads

$$\mathbf{d}_{p_i} = \dot{\lambda}\frac{b}{c}\mathbf{M}_{kin}^D. \tag{5}$$

In Eq. (5) $\mathbf{M}_{kin}^D$ represents a symmetric Mandel-type back stress tensor. The material parameters $b$ and $c$ influence the nonlinear kinematic hardening. In order to consider the rate-dependent behavior, Perzyna viscoplasticity ($\dot{\lambda} = \langle\Phi\rangle^m/\eta$) is applied [9].

It is desirable to formulate the yield function and the evolution equations in terms of tensors which live in the reference configuration. See for a more detailed motivation [8]. After a longer derivation we define the corresponding effective stress tensor

$$\mathbf{Y} = \mathbf{CS} - \mathbf{C}_{p_e}\mathbf{X}, \tag{6}$$

where $X$ defines the back stress tensor in the reference configuration. As in many formulations for plasticity, $\Phi$ denotes the yield function, which in this case is chosen to be of Hill's type:

$$\Phi = \sqrt{\mathbf{Y}^D\cdot\left(\overline{\mathscr{A}}[(\mathbf{Y}^D)^T]\right)} - \sqrt{\frac{2}{3}}(\sigma_y + \mathcal{Q}(1 - e^{-\beta\kappa})). \tag{7}$$

The variable $\mathbf{Y}^D$ in Eq. (7) denotes the deviatoric part of the pulled back Mandel stress tensor, being in general a non-symmetric second order tensor. As in [8], the notation $\overline{\mathscr{A}}[\mathbf{B}]$ is used to describe the application of a fourth order tensor $\overline{\mathscr{A}}$ on a second order tensor $\mathbf{B}$. For an isotropic material, $\overline{\mathscr{A}}$ would be defined as the fourth order identity tensor $\mathcal{I}$.

Damage is introduced in this formulation by means of the Kachanov-Rabotnov concept, where the relation between the local effective stress tensor $\bar{\mathbf{S}}$ and the continuum mechanical second Piola-Kirchhoff stress tensor is given by

$$\mathbf{S} = \bar{\mathbf{S}}(1 - D). \tag{8}$$

Damage $D$ in this case is implemented in the standard, scalar form (see Eq. (9)).

$$D \in [0, 1] \tag{9}$$

Here, $D = 0$ represents an undamaged (virgin) material, while $D = 1$ stands for a complete loss of material stiffness. The ==damage growth criterion of Lemaitre== [10], which is used in this formulation, is given by:

$$\dot{D} = \dot{\lambda}\sqrt{\frac{2}{3}}\frac{1}{1-D}\left(\frac{Y}{s}\right)^{k} H(\kappa - p_D) \tag{10}$$

Variable $Y$ in this formula denotes the damage driving force ($Y = -\partial\psi/\partial D$). The parameters $s$ and $k$ are related to the damage growth rate. The function $H(a)$ stands for the hevyside function:

$$H(\kappa - p_D) = \begin{cases} 0 & \text{if } \kappa < p_D \\ 1 & \text{if } \kappa \geq p_D \end{cases} \tag{11}$$

Utilization of this function ensures damage not to be activated before the accumulated plastic strain $\kappa$ reaches the threshold parameter $p_D$.

$$p_D = \kappa - \frac{\kappa_1 - \kappa_2}{\dot{\epsilon}_1 - \dot{\epsilon}_2}\dot{\epsilon}^{eq}. \tag{12}$$

The parameter $p_D$ depends, as seen from Eq. (12), on the strain rate $\dot{\epsilon}^{eq}$. This model is developed in the framework of finite strains:

$$\dot{\epsilon}^{eq} = \sqrt{\frac{2}{3}\dot{\mathbf{E}} : \dot{\mathbf{E}}} \tag{13}$$

Therefore, the strain rate considered in this model is expressed in terms of the Green Lagrange strain rate $\dot{\mathbf{E}}$ (for detailed information, see [11]). It is assumed here, that the threshold for onset of damage is linearly dependent on the strain rate.

*2.2. Cup deep drawing*

The previously shown material model is applied to the electomagnetic deep drawing process shown in Fig. 1. Due to the symmetry of the problem, only a quarter of the geometry has to be simulated. To reduce the simulation effort, punch, blankholder and die are modeled as rigid bodies (see Fig. 2(a), [12]). The metal sheet is meshed using hexahedral solid elements with reduced integration and a constant number of five elements over the thickness. In order to study mesh convergence, the overall number of elements is varied (see Table 1). The material parameters has been obtained using parameter fitting on an uniaxial tension experiment (see [3] for more details).

In Fig. 2(b) the force displacement curves of meshes four to eight are compared. It can easily be seen, that the results are in a good agreement with the experimental data. Mesh convergence is achieved, when the number of elements exceeds 8840.

The necessity of the implementation of the strain rate-dependence can be seen in Fig. 3. Here, the damage distribution of a rate independent and a rate-dependent model are compared [3]. During quasi static deep drawing, the results are similar. However, the rate-dependence has a huge effect during electromagnetic forming. In both pictures, elements with a damage variable $D = 1$ were deleted. The results of the rate independent simulation suggest material failure during the process. This is not in accordance to experiments as it can be seen, e.g. in [13]. Only

| Mesh number | 1 | 2 | 3 | 4 | 5 | 6 | 7 | 8 |
|---|---|---|---|---|---|---|---|---|
| Number of elements | 1235 | 2295 | 3125 | 5125 | 8840 | 20,145 | 41,245 | 80,580 |

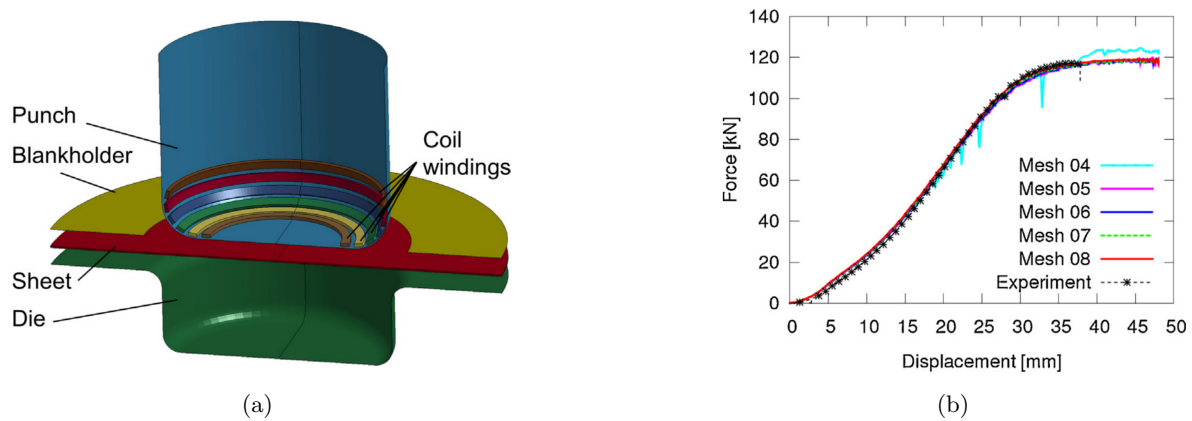**Table 1.** List of overall elements used for convergence studies [3]

(a)                                                 (b)

**Figure 2.** a) Simulation setup and b) comparison of force displacement curves with experimental data [3].



(a) Rate independent damage formulation        (b) Rate dependent damage formulation
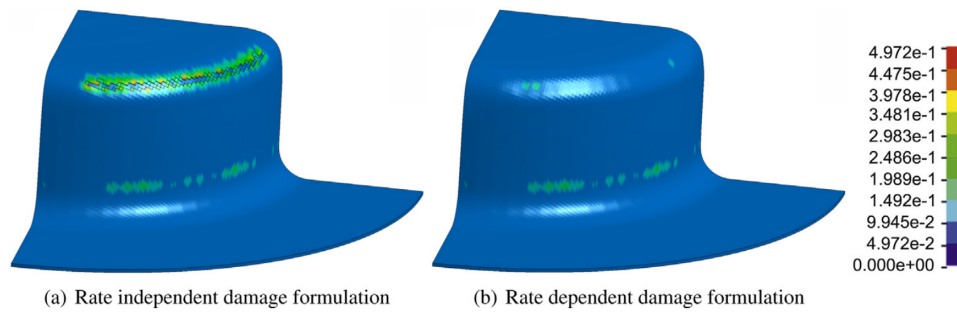
**Figure 3.** Comparison of the damage distribution of rate-dependent and rate-independent model after electomagnetic forming [3]

when rate-dependence is introduced, the material behavior of the experiment can be captured. After the simulation is verified, it is possible to apply an optimization scheme on parameters such as the coil current. For instance, the peak height and impulse length of the current can be optimized with respect to a minimal damage at the end of the deep drawing process or an increased forming limit curve [14].

When simulating a material model including damage behavior, undesired mesh dependencies can occur. A one dimensional exemplification for the so called localization phenomenon is given in the next section.

*2.3. Localization*

Considering a truss with an imperfection and damaging material law, damage will always occur in the element with the imperfection. If it is considered, that dissipation only occurs in the damaged element and dissipation can be related to the damaged volume, one can easily assume that the dissipation of the whole system is dependent on the size of the damaging element. This is called mesh dependence of the solution and is undesired in simulations.

In addition, strains will localize in the aforementioned element (see Fig. 4). Due to damaging of this element, the overall stress is reduced. This means unloading (in the means of a complete stress release) of the undamaged elements while almost all deformation is concentrated in the damaged element. In the extreme case of infinitesimal small elements the final strain distribution would result in a dirac function. While all other elements have been completely unloaded (stress
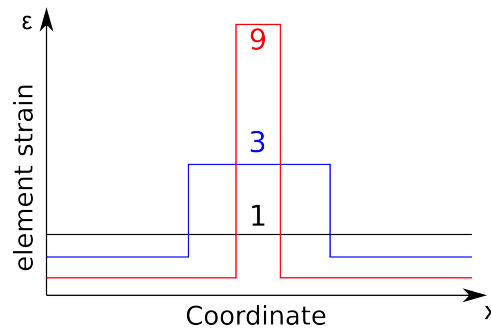
**Figure 4.** Exemplification for a strain localization. Strain distribution for one (black), three (blue) and nine (red) elements over the truss length.

free), all displacement is covered by the middle, damaged element.

In order to avoid this phenomenon, one may use a so-called nonlocal damage formulation such as a gradient-enhanced damage model.

## 3. Gradient-extended damage-plasticity model

In models like the one presented before, the damage variable is treated as an internal variable. The main difference of a gradient extended damage model in comparison to a local model is the assumption that the damage variable $D$ is a field variable. Due to the additional scalar field, this ansatz (see [15] for small deformations and [16] for finite deformations) induces an additional degree of freedom, but also a nonlocality in the damage formulation.

This additional degree of freedom induces an additional (generalized) balance equation and therefore a generalized traction $\Xi$, on which Cauchys lemma ($\Xi = \boldsymbol{\xi} \cdot \boldsymbol{n}$) can be applied to obtain the generalized stress $\xi$. Generalized stress and damage, as well as displacement and stresses, then contribute to the free energy of the system and the power of external forces reads $P = \int_{\partial\Omega}(\boldsymbol{t} \cdot \dot{\boldsymbol{u}} + \Xi\dot{D})da + \int_{\Omega} \boldsymbol{b} \cdot \dot{\boldsymbol{u}}dv$. Application of the principle of virtual work results in the virtual work of the internal forces in Eq. 14.

$$g_{\text{int}} = \int_{\Omega} \boldsymbol{\sigma} \cdot \nabla^s\delta\boldsymbol{u} \, \mathrm{d}\Omega + \int_{\Omega} (a \, \delta D + \boldsymbol{\xi} \cdot \nabla\delta D) \, \mathrm{d}\Omega \tag{14}$$

$$g_{\text{int}} = g_{\text{ext}} \tag{15}$$

In Eq. 14 it is visible, that the standard weak form of finite elements has been extended by a damage related term. Here, $a$ and $\boldsymbol{\xi}$ are internal generalized stresses related to the damage variable. The symbol $\nabla^s$ in this case symbolizes the symmetric part of the gradient. The variables $\delta\boldsymbol{u}$ and $\delta D$ refer to the arbitrary test functions for the displacement field and the damage field, respectively. Note, that $a$ is an abbreviation for the divergence of $\boldsymbol{\xi}$ ($a = div(\boldsymbol{\xi})$). As previously outlined, the standard finite element approach is extended with damage as a new degree of freedom.

Using this model, since the damage evolution depends on the damage gradient, damage and therefore dissipation is distributed also in the surrounding elements. In other words, this strategy introduces an internal length scale like in gradient plasticity theories (see, e.g., [17] for a strain gradient crystal plasticity theory, [18] for the application of gradient plasticity on monotonic and cyclic shearing of laminate micro structures or [19] for comparison of a gradient plasticity model and experimental data).

## 4. Summary

This paper presents a elasto-plastic material model coupled with damage in the regime of finite strains. The model accounts for strain rate sensitivity by means of a strain rate-dependent threshold in the onset of damage. Several simulations based on this material model are carried out. The necessity of the strain rate sensitivity is shown at the example of combined quasistatic-electromagnetic forming.

It is discussed that standard local formulations of damage lead to mesh dependent solutions. A possible solution of this problem is given in terms of a non-local damage formulation.

## References

[1] D.S. Clark and D.S. Wood. The tensile impact properties of some metals and alloys. *ASM TRANS Q*, 42:45–74, 1950.

[2] Y. Kiliclar et al. On the improvement of formability and the prediction of forming limit diagrams at fracture by means of constitutive modelling. In *Material Forming ESAFORM 2012*, volume 504 of *Key Engineering Materials*, pages 29–34. Trans Tech Publications, 4 2012.

[3] Y. Kiliclar et al. Experimental and numerical investigation of increased formability in combined quasi-static and high-speed forming processes. *Journal of Materials Processing Technology*, 237:254–269, 2016.

[4] Y. Kiliclar et al. Finite element analysis of combined forming processes by means of rate dependent ductile damage modelling. *International Journal of Material Forming*, pages 1–12, 2015.

[5] T. Clausmeyer et al. Modeling and finite element simulation of loading-path-dependent hardening in sheet metals during forming. *International Journal of Plasticity*, 63:64–93, 2014.

[6] I. Vladimirov and S. Reese. Anisotropic finite plasticity with combined hardening and application to sheet metal forming. *International Journal of Material Forming*, 1:293–296, 2008.

[7] W. Dettmer and S. Reese. On the theoretical and numerical modelling of armstrong-frederick kinematic hardening in the finite strain regime. *Computer Methods in Applied Mechanics and Engineering*, 193(1):87–116, 2004.

[8] I. Vladimirov et al. Anisotropic finite elastoplasticity with nonlinear kinematic and isotropic hardening and application to sheet metal forming. *International Journal of Plasticity*, 26(5):659–687, 2010.

[9] Piotr Perzyna. Fundamental problems in viscoplasticity. *Advances in applied mechanics*, 9:243–377, 1966.

[10] J. Lemaitre. *A Course on Damage Mechanics*. Springer Science & Business Media, 1992.

[11] I. Vladimirov et al. Anisotropic finite elastoplasticity with nonlinear kinematic and isotropic hardening and application to sheet metal forming. *International Journal of Damage Mechanics*, 26(5):659–687, 2010.

[12] Y. Kiliclar et al. Simulation of electromagnetic forming of a cross-shaped cup by means of a viscoplasticity model coupled with damage at finite strains. In *Key Engineering Materials*, volume 554, pages 2363–2368. Trans Tech Publ, 2013.

[13] A. Brosius et al. Exceeding the forming limit curve with deep drawing followed by electromagnetic calibration. In *5th International Conference on High Speed Forming, April 24th-26th 2012, Dortmund, Germany*, 2012.

[14] Y. Kiliclar et al. Numerical optimization of current parameters in combined electromagnetic-classical forming processes. In *Key Engineering Materials*, volume 651, pages 1406–1411. Trans Tech Publ, 2015.

[15] S. Forest. Micromorphic approach for gradient elasticity, viscoplasticity, and damage. *Journal of Engineering Mechanics*, 135(3):117–131, 2009.

[16] S. Forest. Nonlinear regularization operators as derived from the micromorphic approach to gradient elasticity, viscoplasticity and damage. In *Proc. R. Soc. A*, volume 472, page 20150755. The Royal Society, 2016.

[17] S. Wulfinghoff et al. A gradient plasticity grain boundary yield theory. *International Journal of Plasticity*, 51:33–46, 2013.

[18] S. Wulfinghoff et al. Strain gradient plasticity modeling of the cyclic behavior of laminate microstructures. *ournal of the Mechanics and Physics of Solids*, 79:1–20, 2015.

[19] M. Ziemann et al. Deformation patterns in cross-sections of twisted bamboo-structured au microwires. *Acta Materialia*, 97:216–222, 2015.